第33卷 第5期 发 光 学 报 Vol. 33 No. 5
2012年5月 CHINESE JOURNAL OF LUMINESCENCE May, 2012

Article ID: 1000-7032(2012)05-0519-06

Effect of AlN Interlayer on *a*-plane AlGaN Grown by MOCVD

JIA Hui[1,2], CHEN Yi-ren[1,2], SUN Xiao-juan[1,2], LI Da-bing[1*],
SONG Hang[1], JIANG Hong[1], MIAO Guo-qing[1], LI Zhi-ming[1]

(1. *State Key Laboratory of Luminescence and Applications*, *Changchun Institute of Optics*,
Fine Mechanics and Physics, *Changchun* 130033, *China*;
2. *Graduate University of the Chinese Academy of Sciences*, *Beijing* 100039, *China*)
* *Corresponding Author*, *E-mail*: *lidb@ciomp.ac.cn*

Abstract: The effect of AlN interlayer on strain states and its effect on optical properties of *a*-AlGaN epilayers grown by using metal organic chemical vapor deposition (MOCVD) method are investigated. The strain is characterized by the frequency shift based on Raman spectroscopy measurement. The results show that residual strain in *a*-AlGaN grown on the AlN interlayer is relaxed due to AlN interlayer act as a stable and compliant substrate induced weakening of mechanical strength. Accordingly, the near band edge emission (NBE) peak shows red shift in room temperature photoluminescence measurement. In addition, the introduction of AlN interlayer lead to the red shift of NBE photoluminescence peaks, which can be contribute to the strain determined by Raman spectra.

Key words: *a*-plane AlGaN; AlN interlayer; strain; Raman spectra; PL
CLC number: O47 **Document code**: A **DOI**: 10.3788/fgxb20123305.0519

AlN 插入层对 *a*-AlGaN 的外延生长的影响

贾 辉[1,2], 陈一仁[1,2], 孙晓娟[1,2], 黎大兵[1*],
宋 航[1], 蒋 红[1], 缪国庆[1], 李志明[1]

(1. 发光学及应用国家重点实验室 中国科学院长春光学精密机械与物理研究所, 吉林 长春 130033;
2. 中国科学院 研究生院, 北京 100039)

摘要: 采用有机金属化学气相沉积(MOCVD)在 *r* 面蓝宝石衬底上生长 *a*-AlGaN 外延膜,研究了 AlN 插入层对 *a*-AlGaN 外延膜的应力和光学性质的影响。根据高分辨 X 射线衍射(HRXRD)技术和扫描电子显微镜(SEM)我们可以得到,AlN 插入层有效地提高了 *a*-AlGaN 外延膜的晶体质量并减小了外延膜材料结构的各向异性。由拉曼光谱得到 AlN 插入层的引入减小了 *a*-AlGaN 外延膜的面内压应力,其原因是 AlN 插入层可以当作衬底有效的调制与减小 *a*-AlGaN 外延膜与 *r* 面蓝宝石衬底的晶格失配,从而使 *a*-AlGaN 的面内应力得到适当释放。对室温下的光致发光进行测量得到 AlN 插入层的使用使近带边发射峰(NBE)发生了红移,这可能是由于残余应力的减小引起。

关 键 词: *a*-AlGaN; AlN 插入层; 应力; 拉曼光谱; 光致发光

收稿日期: 2012-02-08; **修订日期:** 2012-03-12
基金项目: 国家基础研究发展计划(2011CB301901); 国家自然科学基金(51072196,51072195,60976011)资助项目
作者简介: 贾辉(1984-), 男, 山东枣庄人, 主要从事 GaN 基材料的外延生长与器件的研究。
E-mail: jia8488ciomp@hotmail.com

1 Introduction

The hexagonal AlGaN system, whose tunable gap depending on the aluminum concentration lies in a typical range of 3.42 ~ 6.2 eV at $T = 300$ K, is extremely attractive for optoelectronic applications[1-3]. Nitride semiconductors epilayers grown along the (0001) c-axis of the wurtzite crystal structure suffer from strong undesirable spontaneous and piezoelectric polarization fields, which give rise to internal electrical fields[4] and impair device performance[5]. A solution to avoid the deleterious polarization-induced electric field effects is to use group-Ⅲ nitride layers in crystal orientations which have no polarization field in the growth direction, and hence across the device active region[6]. Therefore, there is extensive ongoing research toward the growth of "nonpolar" $(11\bar{2}0)$ a-plane and $(1\bar{1}00)$ m-plane. Nonetheless, 'nonpolar' a-plane AlGaN is characterized by high defect density which will affect the following epilayers quality and the surface morphology. Moreover, it is more difficult to grow thick a-plane AlGaN alloys with high Al composition due to the large lattice mismatch, and the different thermal expansion coefficients between substrate and a-plane AlGaN[7].

The lattice mismatch and thermal expansion coefficients of a-plane AlGaN epilayers with respect to the substrate are different from $/\!/ c$ and $\perp c$ -directions. This gives rise to an anisotropic in-plane strain which distorts the basal-plane of the hexagonal unit cell. Strain has an important effect on the performance and reliability of devices, so it is necessary to study the strain and its effect on optical properties in a-plane AlGaN epilayers. In this paper, the effect of AlN interlayer on the strain state of subsequent a-plane AlGaN layers has been investigated. Furthermore, the strain effect on optical characteristics of the a-plane AlGaN was discussed as well.

2 Experiments

The a-plane AlGaN alloys were grow on 5.08 cm (2 in) r-plane sapphire by low-pressure metal-organic chemical vapor deposition (LP-MOVPE) with an in-situ optical reflectance monitor. During the growth, trimethylgallium (TMGa) and trimethylaluminum (TMAl) were used as group Ⅲ source materials, ammonia (NH_3) as the group Ⅴ source material, and high purity hydrogen as a carrier gas. Two types of a-plane AlGaN layers grown on r-plane sapphire were studied: (a) 1 μm-thick a-plane AlGaN layers grown directly on sapphire substrate without any underlying layer for sample A, (b) 1 μm-thick a-plane AlGaN layer was grown with a high-temperature AlN interlayer for sample B. Prior to growth, nitridation was performed in NH_3 ambient at 1 100 ℃ for 5 min after thermally cleaning a sapphire substrate in H_2 ambient for 10 min. The pressure was then lowered to 3 000 Pa and a 500 nm thick AlN interlayer was grown at 1 250 ℃ for sample B. The pressure was raised to 5 332 Pa and the temperature lowered to 1 160 ℃ for the growth of a 1 μm thick a-plane AlGaN layer.

In this study, high-resolution X-ray diffraction (HRXRD), and scanning electron microscope (SEM) were performed to study the structural properties, crystalline quality and surface morphology of the a-plane AlGaN epilayers. The Raman spectra were used to analyze the residual strain of a-plane AlGaN epilayers using a 488 nm line from the YAG laser with $x(y, y+z)-x$ scattering geometry at room temperature. The photoluminescence (PL) of all the samples were obtained by using the fourth frequency of a YAG laser (266 nm) on the a-plane AlGaN samples at room temperature (300 K).

3 Results and Discussion

The samples surface present prominent striation along the c-axis, as shown by SEM micrography in Fig. 1. The features on the surface of the samples have been reported in reference [8] and are attributed to the more complex growth mechanism on nonpolar and semipolar surfaces, where growth proceeds at different rates and the different migration lengths of adatoms along the m- and c-directions[9].

But the key point to understand these results is the anisotropy of the in-plane strain in a-plane AlGaN epilayers grown on r-plane sapphire. Comparing with the sample A, the AlN interlayer growth method

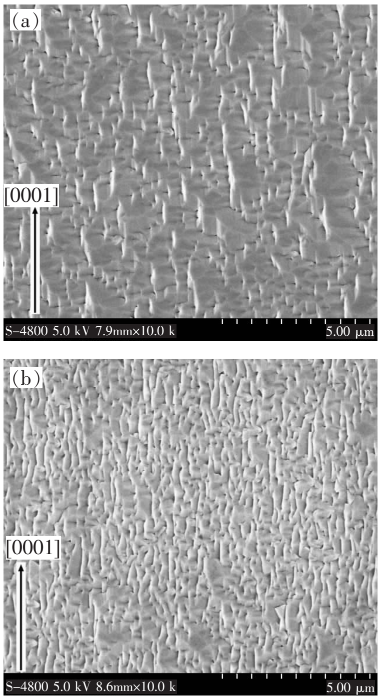

Fig. 1　SEM images of *a*-plane AlGaN without (a) /with (b) HT AlN interlayer

leads to smoother surface for *a*-plane AlGaN and higher density of smaller pits. The optimal AlN interlayer is thought to provide the good orientation seeds layer for the subsequent AlGaN growth. The AlN interlayer is found to be effective for the growth of *a*-plane AlGaN.

Fig. 2 shows corresponding data from measurements under symmetrical diffraction geometry and various orientations of the diffraction plane. Craven *et al*. examined the epitaxial relationship in the *a*-plane GaN/*r*-plane sapphire system. A combination of X-ray diffraction and convergent beam electron diffraction (CBED) was used to explicitly define the epitaxial relationship in the *a*-plane GaN/*r*-plane Al_2O_3 system as follows: $[0001]_{GaN} \parallel [1\bar{1}01]_{sapphire}$ and $[1\bar{1}00]_{GaN} \parallel [11\bar{2}0]_{sapphire}$[10]. Both the *a*-plane AlGaN epilayers show an in-plane anisotropy in the crystalline mosaicity. The $(11\bar{2}0)$ ω-FWHM value is maximum when the scattering plane is along *c*-direction ($Q_x \parallel [0001]$) and is minimum when the scattering plane is along *m*-direction ($Q_x \parallel [1\bar{1}00]$) for the sample A, but it is exactly opposite in sample B. The crystalline anisotropy observed on semipolar and nonpolar AlGaN samples can be attributed to the domains sizes. The broadening of the XRD rocking curve can be affected by the coherence scattering length and by the tilt scattering disorder. To evaluate separately the effect of each contribution further work is needed, including Williamson hall plot measurements or reciprocal space mapping studies. However, in our case, we assume that the dominant contribution to the anisotropy is due to the scattering coherence length anisotropy. If a difference of $(11\bar{2}0)$ FWHM values between *c*- and *m*- direction ($|FWHM_{c\text{-axis}} - FWHM_{m\text{-axis}}|$) is used as a mark for the degree of in-plane structural anisotropy. It is clearly that AlN interlayer methods benefit the decreased structural anisotropy of *a*-plane AlGaN, as shown in Fig. 2. Anisotropic feature marked as a W-shape dependence on the azimuth angle was observed for sample without AlN interlayer. However, for sample B, an inverse M-shape distribution is observed: the ω-FWHM measured in the $[1\bar{1}00]$ direction is higher than that in the [0001] direction, as shown in Fig. 2 (inverse triangle). The transformation to the inverse feature of anisotropy (from W- to M- shape) has also been observed in *a*-plane GaN[7,11,20]. The reason for this transformation is not clear. In our case, it may be attributed to the AlN interlayer growth under high temperature and the AlN interlayer like stripe masks applied in epitaxial lateral overgrowth[7].

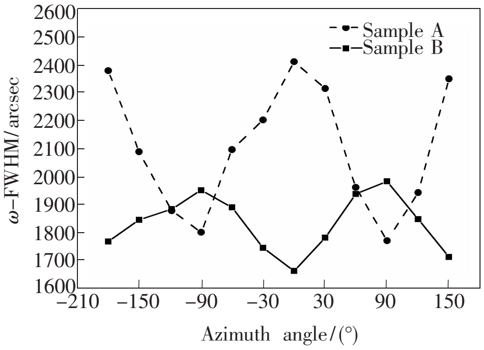

Fig. 2　Full width at half maximum values of the $(11\bar{2}0)$ rocking curves measured under different azimuth angles

It is well known that the vibrational frequency shift of phonon modes is linearly dependent on the strain. Raman spectroscopy was used to identify the phase purity and strain as well[11-12]. According to group theory[13], AlGaN has eight sets of optical phonon modes at Γ point of the Brillouin zone, A_1 (TO, LO) + $2B_1$ + E_1(TO, LO) + $2E_2$. Both B_1 and E_2 consist of two modes of low and high frequency. Among them, A_1 and E_1 modes are both Raman and infrared (IR) active, while the two E_2^{modes} (E_2^{low} and E_2^{high}) are only Raman active, and the two B_1 modes are neither Raman nor IR active (silent modes). Thus, six optical modes, *i. e.*, A_1(LO), A_1(TO), E_1(LO), E_1(TO), E_2^{high}, and E_2^{low}, can be observed for the first-order Raman scattering. Raman spectra were obtained to study the samples in the various back-scattering configurations. Here $x // [11\bar{2}0]$, $y // [1\bar{1}00]$ and $z // [0001]$. The room-temperature Raman spectra for the *a*-plane AlGaN epilayer measured with the polarization of incident light vertical to the *c*-axis in our experiment. Therefore, only A_1(TO), E_1(TO), and E_2^{high} modes are allowed according to the Raman selection rule[14].

Fig. 3 shows the room-temperature Raman spectra for the *a*-plane AlGaN layer measured with the polarization of incident light vertical to the *c*-axis. For sample B, three peaks marked with stars correspond to the A_1(TO), E_2^{high} and E_1(TO) modes for AlN interlayer, respectively. Results show that the intensity of the E_2^{high} mode is the strongest. The spectra in the scattering configurations corresponding to E_2^{high} and E_1(TO) phonons have identical shapes, it is impossible to distinguish one phonon from the other within the A_1 composition range of 0.28 ~ 0.7 for AlGaN[15-17]. The position of A_1(TO) phonons also cannot be distinguished, because it merged into the E_2^{high} and E_1(TO) phonons. There is also a peak at 418 cm^{-1} in Fig. 3, which is from the *r*-plane sapphire substrate. All the observed phonon modes in the $x(y, y+z)-x$ configurations are in good accordance with the selection rules. According to the calculation and experimental results of Demangeot *et al.*[18], the Raman shift of nitrides is closely related to the strain in the epilayer. They pointed out that the Raman shift will shift to higher frequency as a result of compressive strain and to lower frequency as a result of tensile strain. A compressive in-plane strain is expected in the *a*-plane AlGaN film, due to the lattice mismatch of GaN in the $[\bar{1}100]$ and [0001] directions of −2.4% and −3.9%, respectively, relative to AlN; and −16% and −1%[19-21], respectively, relative to the sapphire substrate. These values show compressive strain in the two in-plane directions of *a*-plane AlGaN film, which correspond to blue-shift of the Raman shift. The results show that the AlN interlayer can effectively reduced the compressive strain in *a*-plane AlGaN film as shown in Fig. 3, because the AlN interlayer modulates and reduces the mismatch between *a*-plane AlGaN and sapphire, and act as a stable and compliant substrate induced weakening of mechanical strength[22].

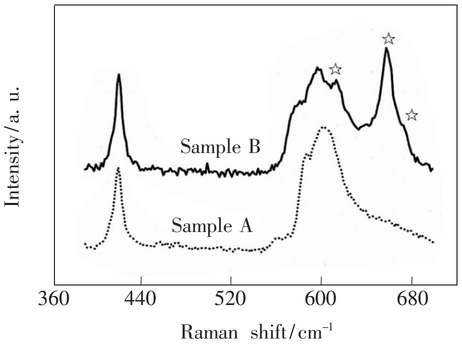

Fig. 3 Raman spectra of *a*-plane AlGaN for sample A and sample B

The room temperature PL spectrum from sample A and sample B is shown on Fig. 4. At room temperature only the near band edge emission (NBE) could be detected.

The FWHM of PL spectrum were 10.4 nm for the sample B and 14.8 nm for the sample A. The result revealed that the crystalline quality of *a*-plane AlGaN is improved by AlN interlayer which consistent with the SEM and XRD results. On the other hand, the NBE peak in the *a*-plane AlGaN layers slightly shift from 296.8 nm to 302.5 nm. We estimate a red shift of 78 meV of the bandgap with respect to AlN interlayer which would suggest even a compressive in-plane strain in the *a*-plane AlGaN layers is reduced[23]. It is well known that the residual strain can effect the energy bandgap, a tensile strain will result in a decrease of energy bandgap while a compressive strain cause an increase of bandgap[24]. In this case the strain-induced bandgap shift, which

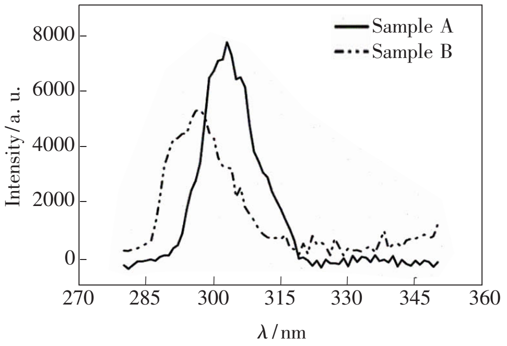

Fig. 4 Photoluminescence spectra of *a*-plane AlGaN for sample A and sample B

generally depends on all three strain components, cannot be predicted as straightforward as in the polar AlGaN[21,25-26]. The strain anisotropy of the nonpolar AlGaN can result from: 1) a difference of the lattice parameters mismatch between AlGaN and sapphire in *c*- and *m*-directions, 2) a different level of relaxation in these two directions, 3) not the same difference thermal expansion coefficients between AlGaN and sapphire in two directions.

Thus the results of the photoluminescence studies are consistent with the residual strain in *a*-plane AlGaN grown on *r*-plane sapphire as inferred from Raman data. Furthermore, due to the blue-shift of the Raman shift, which correspond to the AlN interlayer reduces the compressive strain in *a*-plane AlGaN film grown on sapphire.

4 Conclusion

In summary, the XRD, Raman spectra, and PL spectra of *a*-plane AlGaN/Al_2O_3 (sample A) and *a*-plane AlGaN/AlN/Al_2O_3 (sample B) have been measured and investigated. It is observed the AlN interlayer is beneficial to improve the quality and benefits the reduction of the structural and strain anisotropic distribution of the *a*-plane AlGaN. The strain was characterized by the frequency shift in Raman spectroscopy measurement. There is compressive strain in the epitaxial AlGaN epilayers of both samples A and B due to the mismatch between AlGaN and Al_2O_3, while AlN interlayer modulates and reduces the compressive strain. In addition, the near band edge emission (NBE) peak shows red shift in room temperature photoluminescence (PL) measurement, which correspond to the AlN interlayer reduces the compressive strain.

References:

[1] Monroy E. Wide-band gap semiconductor ultraviolet photodetectors semicond [J]. *Sci. Techno.*, 2003, 18(2):R33-R51.

[2] Liao Meiyong, Jose Alvarez, Yasuo Koide. Thermal stability of diamond photodiodes using tungsten carbide as Schottky contact [J]. *Jpn. J. Appl. Phys.*, 2005, 44:7191-7206.

[3] Razeghi M, Rogalski A. Semiconductor ultraviolet detectors [J]. *J. Appl. Phys.*, 1996, 79(10):7433-7473.

[4] Im J S, Kollmer H, Off J, *et al.* Reduction of oscillator strength due to piezoelectric fields in GaN/$Al_xGa_{1-x}N$ quantum well [J]. *Phys. Rev.* B, 1998, 57(16):R9435-R9348.

[5] Cingolani R, Botchkarev A, Tang H, *et al.* Spontaneous polarization and piezoelectric field in GaN/$Al_{0.15}Ga_{0.85}N$ quantum wells: Impact on the optical spectra [J]. *Phys. Rev.* B, 2000, 61(4):2711-2715.

[6] Paskova T. Development and prospects of nitride materials and devices with nonpolar surfaces [J]. *Phys. Status Solidi* B, 2008, 245(6):1011-1025.

[7] Tsuda M, Furukawa G, Honshio A, *et al.* Anisotropically biaxial strain in *a*-plane AlGaN on GaN grown on *r*-plane sapphire [J]. *Jpn. J. Appl. Phys.*, 2006, 45:2509-2513.

[8] Wang H M, Chen C Q, Gong Z, *et al.* Anisotropic structural characteristics of ($11\bar{2}0$) GaN templates and coalesced epitaxial lateral overgrown films deposited on ($10\bar{1}2$) sapphire [J]. *Appl. Phys. Lett.*, 2004, 84(4):499-501.

[9] Sasaki T, Zembutsu S. Substrate-orientation dependence of GaN single-crystal films grown by metalorganic vapor-phase epitaxy [J]. *J. Appl. Phys.*, 1987, 61(7):2533-2540.

[10] Craven M D, Lim S H, Wu F, *et al.* Structural characterization of nonpolar ($11\bar{2}0$) *a*-plane GaN thin films grown on ($1\bar{1}02$) *r*-plane sapphire [J]. *Appl. Phys. Lett.*, 2002, 81(3):469-471.

[11] Gao H, Yan F, Li J, *et al.* Polarized Raman scattering studies of nonpolar *a*-plane GaN films grown on *r*-plane sapphire

substrates by MOCVD [J]. *Phys. Status Solidi* A, 2006, 203(15):3788-3792.

[12] Wei T B, Duan R F, Wang J X, *et al.* Microstructure and optical properties of nonpolar *m*-plane GaN films grown on *m*-plane sapphire by hydride vapor phase epitaxy [J]. *Jpn. J. Appl. Phys.*, 2008, 47:3346-3349.

[13] Hayers W, Laudon R. *Scattering of Light by Crystals* [M]. Edited by Wiley, New York: UMich, 1978:275-280.

[14] Hiroshi Harima. Properties of GaN and related compounds studied by means of Raman scattering [J]. *J. Phys.: Condens. Matter*, 2002, 14:R967-R993

[15] Davydov V Yu, Goncharuk I N, Smirnov A N, *et al.* Composition dependence of optical phonon energies and Raman line broadening in hexagonal $Al_xGa_{1-x}N$ alloys [J]. *Phys. Rev.* B, 2002, 65(12):125203-1-13.

[16] Cros A, Angerer H, Handschuh R, *et al.* Raman study of the optical phonons in $Al_xGa_{1-x}N$ alloys [J]. *Solid State Commun.*, 1997, 104(1):35-39.

[17] Demangeot F, Groenen J, Frandon J, *et al.* Coupling of GaN- and AlN-like longitudinal optic phonons in $Ga_{1-x}Al_xN$ solid solutions [J]. *Appl. Phys. Lett.*, 1998, 72(21):2674-2676.

[18] Demangeot F, Frandon J, Renucci M A, *et al.* Raman determination of phonon deformation potentials in α-GaN [J]. *Solid State Commun.*, 1996, 100(4):207-210.

[19] Li Dongsheng, Chen H, Yu H B, *et al.* Effects of carrier gas on the strain of *a*-plane GaN films grown on *r*-plane sapphire substrates by metalorganic chemical vapor deposition [J]. *Journal of Crystal Growth*, 2004, 263(1-4):76-79.

[20] Morkoç H. *Nitride Semiconductors and Devices* [M]. Edited by Springer, Berlin: Wiley-vch, 1999:98-101.

[21] Ghosh S, Misra P, Grahn H T, *et al.* Polarized photoreflectance spectroscopy of strained *a*-plane GaN films on *r*-plane sapphire [J]. *J. Appl. Phys.*, 2005, 98(2):026105-1-3.

[22] Chen Chengzhao, Liao Linghong, Li Cheng, *et al.* Role of Ge interlayer in the growth of high-quality strain relaxed SiGe layer with low dislocation densit [J]. *Appl. Surf. Sci.*, 2011, 257(7):2818-2821

[23] Kisielowski C, Kruger J, Ruvimov S, *et al.* Strain-related phenomena in GaN thin films [J]. *Phys. Rev.* B, 1996, 54(24):17745-17753.

[24] Willian G P, Zheleva T, Bremser M D, *et al.* Correlation of biaxial strains, bound exciton energies, and defect microstructures in GaN epilayers grown on AlN/6H-SiC(0001) substrates [J]. *J. Electronics Material.*, 1997, 36:224-227.

[25] Paskov P P, Paskova B, Haskell B A, *et al.* Photoluminescence of *a*-plane GaN: comparison between MOCVD and HVPE grown layers [J]. *Phys. Stat. Sol.* C, 2006, 3(6):1499-1502.

[26] Zheng Dongmei, Wang Zongchi, Xiao Ronghui. Hydrogenic donor impurity states in a cylindrical wurtzite GaN quantum dot [J]. *Chin. J. Lumin.* (发光学报), 2010, 31(5):628-634 (in Chinese).